

Dark Photon Polarimetry

Fiesta Ting Yan Leung,^{1,*} Tao Liu,^{1,†} Sida Lu,^{2,‡} Jing Ren,^{3,4,§} Cheuk Kan Kelvin Yue,^{1,¶} and Kaifeng Zheng^{1,**}

¹*Department of Physics and Jockey Club Institute for Advanced Study,*

The Hong Kong University of Science and Technology, Hong Kong S.A.R., China

²*Institute for Advanced Study, The Hong Kong University of Science and Technology,
Clear Water Bay, Kowloon, Hong Kong S.A.R., China*

³*Institute of High Energy Physics, Chinese Academy of Sciences, Beijing 100049, China*

⁴*Center for High Energy Physics, Peking University, Beijing 100871, China*

We propose detecting dark photon (DP), a major candidate for wave dark matter, through polarimetry. The DP can modify Maxwell’s equations, due to its kinetic mixing with regular photon, inducing an oscillating component in the electromagnetic field. This may leave an imprint in polarimetric light signals, characterised by a distinctive wave pattern in spacetime. As a demonstration, we apply this methodology to investigate ultralight DP produced through the superradiance of supermassive black holes. Then using the polarimetric measurements of the radiation from M87* at the Event Horizon Telescope, we show that all Stokes parameters can serve as a probe in conducting this task. Especially, the absence of significant temporal variation in the linear-polarisation position angle of the M87* images allows us to set novel limits on the photon-DP mixing parameter over the rarely-explored DP mass range of 10^{-22} – 10^{-20} eV, with the best reach of $\sim 10^{-8}$ achieved at $\sim 10^{-20.2}$ eV. Given the universality of its underlying physics, we expect the DP polarimetry to be broadly applied for the DP detection in laboratory experiments and astronomical observations.

INTRODUCTION

Despite compelling evidence [1–3] for their existence, the nature of dark matter (DM) remains elusive. The null results from direct DM detections [4–6] and complementary searches at the Large Hadron Collider challenge the conventional model of weakly interacting massive particles, where the DM mass is typically at electroweak scale, advocating for alternative models. Among the suggested possibilities, bosonic particles with a mass of $\lesssim 1$ eV emerge as an intriguing DM candidate. With their wave nature overshadowing their particle characteristics, these bosons are often referred to as “wave DM” (for a review, see, e.g., [7]) and possess unique astrophysical and cosmological implications [8–14].

One representative example of wave DM is dark photon (DP) [15], a massive Abelian vector boson (A') that interacts with the Standard Model of particle physics through a kinetic mixing with the regular photon (A), described by the Lagrangian $\mathcal{L} \supset -\frac{\varepsilon}{2} F'_{\mu\nu} F^{\mu\nu}$. Here, $F'_{\mu\nu}$ and $F^{\mu\nu}$ represent the field strengths of the DP and the photon, and ε is their kinetic mixing parameter. In last decades, extensive experiments and observations have been taken and many novel methods have been proposed for investigating the DP non-gravitational properties [16–23]. These efforts primarily leverage mixing-induced DP-photon conversions and interactions of the DP with charged particles, yielding stringent constraints on its mixing parameter across a wide mass range (see, e.g., [24], for a summary of existing limits). However, the ultralight mass region of $\lesssim 10^{-18}$ eV [25], including the well-known fuzzy DM scenario [11, 26] which offers a potential solution to the “small-scale” structure problems, remains rarely explored.

To address this challenge, in this Letter we propose detecting the DP through polarimetry. This optical methodology has been broadly utilised to detect axions or axion-like particles, another prominent candidate for wave DM. When linearly polarised light travels across an axion field or DM halo, its polarisation position angle (PA) can be rotated due to a topological effect induced by the axion Chern-Simons coupling. This phenomenon is commonly referred to as “cosmic birefringence (CB)” [27, 28]. Over the past decades, various polarimetric observation tools or methods have been developed to measure this effect, including Cosmic Microwave Background (CMB) [29–31], pulsar polarisation arrays [32, 33], supermassive black holes (BHs) [34–37], and Crab Nebula [38, 39], etc.

In contrast to the case of the axion or axion-like DM, the DP polarimetry is based on the effective current in the Maxwell’s equations which arises from the photon-DP kinetic mixing. This effect induces an oscillating component in the electromagnetic (EM) field, and in the magneto-optic media (e.g., plasma) may leave an imprint in the polarimetric light signals such as Faraday rotation (FR) and dichroism, characterised by a specific wave pattern in spacetime. Given the universality of its underlying physics, the DP polarimetry can be applied for the DP detection in both laboratory experiments and astronomical or cosmological observations. For demonstration, below we will consider supermassive BHs which are usually surrounded by dense thermal plasma as a platform for performing this investigation.

The ultralight DP is known to be subject to superradiance near a spinning or Kerr BH, by draining its energy and angular momentum. When their Compton wavelength is comparable to the BH horizon, requiring the BH to be supermassive, a macroscopic cloud of DPs

can be exponentially populated, forming a coherent state. The cloud profiles are characterised by a set of quantum numbers (n, j, l, m) , similar to electron eigenstates of a hydrogen atom. Thus, such a system is often dubbed “gravitational atom” [40]. The signatures of the ultralight DP thus can be sought through polarimetric observations of the supermassive BHs such as the one at the center of the galaxy Messier 87 (M87*) using the Event Horizon Telescope (EHT) [41]. Below, while emphasizing the role of the FR observable in constraining the photon-DP kinetic mixing, we will show that other Stokes parameters can also serve as a sensible probe in conducting this task.

DARK PHOTON POLARIMETRY AND BLACK HOLES

The Maxwell’s equations with a photon-DP kinetic mixing are given by

$$\partial_\mu F^{\mu\nu} = -(J^\nu + J'^\nu). \quad (1)$$

Here, J^ν denotes a regular EM current, and $J'^\nu = -\varepsilon\mu^2 A'^\nu + \mathcal{O}(\varepsilon^2)$ is induced by the DP through its kinetic mixing with the photon. Since these equations are linear, the components of the EM field strength sourced by J'^ν can be isolated from the others when studying the DP polarimetry.

For gravitational atoms with a DP cloud, the DP field in Eq. (1) should be interpreted as the cloud profile. To the leading order of gravitational fine-structure constant, namely $\alpha = GM\mu$, the profile for the fastest-growing mode $(n, j, l, m) = (1, 1, 0, 1)$ is given by [42, 43]

$$\begin{aligned} A'_0 &= \frac{\sqrt{M_c}}{\sqrt{\pi}\mu^2 r_c^{5/2}} e^{-r/r_c} \sin\theta \sin(\omega t - \varphi + \phi_0), \\ \vec{A}' &= -\frac{\sqrt{M_c}}{\sqrt{\pi}\mu r_c^{3/2}} e^{-r/r_c} \{\cos(\omega t + \phi_0), \sin(\omega t + \phi_0), 0\}. \end{aligned} \quad (2)$$

Here, r is understood as the “ $r - r_+$ ” in the Boyer-Lindquist coordinate system, with r_+ being the Kerr BH horizon, the direction of $\theta = 0$ is aligned with the BH spinning axis, and φ is azimuthal angle. Additionally, $r_c = r_g/\alpha^2 = 1/(GM\mu^2)$ is the gravitational Bohr radius, with M being the BH mass and $r_g = GM$ representing the half Schwarzschild radius, $M_c \sim 0.1\alpha M$ is the DP cloud mass for $\alpha \ll 1$, $\omega \simeq \mu(1 - \alpha^2/2)$ is the DP eigenenergy, and ϕ_0 is a random constant phase. We will take this profile below for the proof of concept.

Given the J'^ν , the DP-induced EM fields are then solved to be

$$\begin{aligned} \vec{B}_{A'}(t, \vec{x}) &= \int dt' d\vec{x}' G(t, \vec{x}; t', \vec{x}') \left(\nabla \times \vec{J}'(t', \vec{x}') \right), \\ \vec{E}_{A'}(t, \vec{x}) &= - \int dt' d\vec{x}' G(t, \vec{x}; t', \vec{x}') \left(\nabla J'^0 + \partial_{t'} \vec{J}'(t', \vec{x}') \right). \end{aligned} \quad (3)$$

Here, $G(t, \vec{x}; t', \vec{x}')$ is Green’s function (GF), with (t', \vec{x}') and (t, \vec{x}) denoting the positions of the source or the DP cloud and the EM field, respectively. As $A'_0 \sim \alpha|\vec{A}'|$ and $1/r_c \sim \alpha\mu$, the contribution of $\nabla J'^0$ to $E_{A',i}(t, \vec{x})$ can be neglected.

A rigorous treatment of the GF requires summing the eigenfunctions in the Kerr metric after applying separation of variables, as illustrated in [44]. However, the signal signature primarily forms on the BH accretion disk, whose inner edge is located outside the photon sphere and not very close to the event horizon ($r_+ \sim r_g$). The metric in this area differs from that of flat spacetime only up to a factor of $\sim \mathcal{O}(1)$. Therefore, we will take the GF in the flat spacetime as a leading-order approximation in this exploratory study. Moreover, the current J' is exponentially suppressed in the region of $r > r_c$, so we expect the PA polarimetry to be particularly relevant for $r_g < r \ll r_c$. In this context, the DP-induced EM fields are approximately given by:

$$\begin{aligned} B_{A',r} &= 0, \\ B_{A',\theta} &\approx 0.2\varepsilon\alpha^{11/2}\Lambda \left(\frac{r}{r_g} \right) \cos(\omega t - \varphi + \phi_0), \\ B_{A',\varphi} &\approx 0.2\varepsilon\alpha^{11/2}\Lambda \left(\frac{r}{r_g} \right) \cos\theta \sin(\omega t - \varphi + \phi_0), \\ E_{A',r} &\approx 0.3\varepsilon\alpha^{7/2}\Lambda \sin\theta \sin(\omega t - \varphi + \phi_0), \\ E_{A',\theta} &\approx 0.3\varepsilon\alpha^{7/2}\Lambda \cos\theta \sin(\omega t - \varphi + \phi_0), \\ E_{A',\varphi} &\approx -0.3\varepsilon\alpha^{7/2}\Lambda \cos(\omega t - \varphi + \phi_0). \end{aligned} \quad (4)$$

Here, $B_{A',r}$ is zero because the axial symmetry of \vec{J}' renders it curl-free in the radial direction. The characteristic α scalings of $E_{A'}$ and $B_{A'}$, *i.e.*, $B_{A'} \sim \alpha^2 E_{A'} \propto \alpha^{11/2}$, arise from the cancellation of lower-order terms in the small α expansion, different from those at $r \sim r_c$. $\Lambda = 1/(r_g\sqrt{\pi G})$ is a factor characterising the strength of the DP-induced EM field for a given gravitational atom. Its value is solely determined by the BH mass and is equal to $7.3 \times 10^9 \text{G}$ or $2.2 \times 10^{14} \text{V/m}$ for the M87*, where $M \approx 6.5 \times 10^9 M_\odot$.

The BH accretion disk is not in rest in the observer frame. It is convenient then to denote the total EM field strength in the plasma frame as $\vec{\mathcal{E}}$ with $\mathcal{E} = |\vec{\mathcal{E}}|$ and $\vec{\mathcal{B}}$ with $\mathcal{B} = |\vec{\mathcal{B}}|$. Then in the direction transverse to the boost, the DP-induced components $\vec{\mathcal{E}}_{A'}$ and $\vec{\mathcal{B}}_{A'}$ are related to $\vec{B}_{A'}$ and $\vec{E}_{A'}$ through the Lorentz transformation

$$\begin{aligned} \mathcal{E}_{A'} &\sim \gamma_p(\beta_p B_{A'} + E_{A'}), \\ \mathcal{B}_{A'} &\sim \gamma_p(-\beta_p E_{A'} + B_{A'}), \end{aligned} \quad (5)$$

where β_p and γ_p are plasma velocity and boost factor in the observer frame. Notably, the strong DP-induced electric field could be efficiently screened by plasma at the BH disk. Take the M87* as an example. Its environmental plasma is relativistic, with a thermal temperature

$\sim 10^{11}$ K and an electron number density $\sim 10^5/\text{cm}^3$, which results in a Debye length of $\lambda_D \sim 10 - 100$ m. This implies that in the M87* plasma the DP-induced electrostatic effect can persist only a distance much shorter than the BH horizon and the cloud geometric size. The strength of the DP-induced electric field in the plasma, as a yield of the DP-induced effective charge inside Debye sphere, is thus negligibly small. So the electric field in the observer frame $\vec{E}_{A'}$ is estimated to be $\sim -\beta_p \vec{B}_{A'}$, which further contributes to $\vec{B}_{A'}$ by an amount $\sim -\beta_p^2 \vec{B}_{A'}$. As β_p is $\sim \mathcal{O}(0.1)$ for the M87*, finally we have $\vec{B}_{A'} \sim \gamma_p \vec{B}_{A'}$. This is consistent with the assumptions taken for the ideal magnetohydrodynamics simulation in Ref. [45]. Also, the potential synchrotron radiation and cascade production of electron-positron pairs caused by the unscreened DP-induced electric field [43] may not be efficient.

The $\vec{B}_{A'}$ field can modify radiative transfer in the BH plasma in an oscillatory way, leaving an imprint in the time series of its polarimetric data. Generally, the polarimetric features of a radiation field are described by Stokes parameters (I, Q, U, V) , where the linear polarization PA is given by $\chi \equiv \frac{1}{2} \arg(Q + iU)$. These parameters evolve during light propagation according to the radiative transfer equation [46, 47]:

$$\frac{d}{ds} \begin{pmatrix} I \\ Q \\ U \\ V \end{pmatrix} = \begin{pmatrix} j_I \\ j_Q \\ j_U \\ j_V \end{pmatrix} - \begin{pmatrix} \alpha_I & \alpha_Q & \alpha_U & \alpha_V \\ \alpha_Q & \alpha_I & \rho_V & \rho_U \\ \alpha_U & -\rho_V & \alpha_I & \rho_Q \\ \alpha_V & -\rho_U & -\rho_Q & \alpha_I \end{pmatrix} \begin{pmatrix} I \\ Q \\ U \\ V \end{pmatrix}, \quad (6)$$

where $j_{I,Q,U,V}$ are the plasma emissivity coefficients, $\alpha_{I,Q,U,V}$ are the plasma absorption coefficients, and $\rho_{I,Q,U,V}$ are the Faraday mixing coefficients. It is convenient to align the U parameter with the magnetic field such that $j_U = \alpha_U = \rho_U = 0$ [48]. The remaining coefficients depend on the total \vec{B} [47] and hence are subject to a mediation by the DP-induced $\vec{B}_{A'}$ component.

Let us consider the weak- \vec{B} limit of radiation frequency $\nu \gg \nu_B = \frac{eB}{2\pi m_e}$, which applies for most of the parameter space we are exploring. For thermal plasma, the j , α and ρ coefficients with a non-“ U ” subscript are proportional to the plasma electron density n_e . The emission coefficients contain a factor of $\exp[-(\frac{2T\nu}{4\nu_c})^{1/3}]$, where $\nu_c = 3 \sin \theta_B \theta_e^2 \nu_B / 2$ is a characteristic frequency, with $\theta_e = T/m_e$, and θ_B is the angle between the light wave vector and the magnetic field direction. The absorption coefficients are determined by Kirchoff’s Law $j_{I,Q,U,V} = f_\nu \alpha_{I,Q,U,V}$, where $f_\nu = \nu^3 / (e^{\nu/T} - 1)$ is a blackbody function [49]. Thus, these coefficients are exponentially suppressed for a weak \vec{B} field. On the other hand, the Faraday mixing coefficient ρ_V is linear in \mathcal{B} , up to a mild logarithmic \mathcal{B} term, and has a temperature dependence of $\propto \theta_e^{-2} \log \theta_e$ for $\theta_e \gg 1$. Another coefficient ρ_Q is $\propto \mathcal{B}^2 \theta_e$ and enhanced by the plasma temperature

in the same case [48]. As the M87* plasma is relativistic, this implies that while the DP-induced $\vec{B}_{A'}$ generates an oscillating imprint in FR, it may convert the U parameter to the V parameter, yielding an additional effect of dichroism.

POLARIMETRIC CONSTRAINTS ON PHOTON - DARK PHOTON KINETIC MIXING

Next, we will apply the polarimetry for detecting the ultralight DP, utilising the EHT polarimetric data of M87*. The evolution of the Stokes parameters within the DP cloud is tracked using the public relativistic polarised radiative transport code IPOLE [50–52], by incorporating the DP-induced oscillating component into the EM field. Simultaneously, the radiatively inefficient accretion flow model [53] is adopted:

$$n_e = n_e^0 \left(\frac{r + r_+}{r_g} \right)^{-1.1} e^{-\frac{\cot^2 \theta}{2H^2}}, \quad (7)$$

to describe the environmental electron number density of the M87*. Here, we set $H = 0.3$ and $n_e^0 = 3.4 \times 10^5/\text{cm}^3$ to ensure that the image intensity predicted by IPOLE matches with the EHT observations, with the effects of the DP cloud turned off.

Let us consider the FR observation at the EHT first. Four polarimetric images of M87* were captured on April 5, 6 and April 10, 11 of 2017, respectively [54]. For sensitivity analysis, we introduce a universal sky plane for all M87* images using a polar coordinate system $(\tilde{r}, \tilde{\varphi})$. The pole is positioned at the centre of the M87* image, with the polar axis aligned with the spin projection of M87* onto the plane. The intensity-weighted average PA for the a -th image, sorted chronologically, is defined as

$$\langle \chi(\tilde{\varphi}, t) \rangle_i^a = \frac{1}{2} \arg(\langle (Q \times I)_i^a + i(U \times I)_i^a \rangle), \quad (8)$$

where, as noted in [54], the average is performed over $\tilde{\varphi}$ within its i -th bin, with a width of 10° . We can define an observable then to measure the variation of $\langle \chi(\tilde{\varphi}, t) \rangle$ over two successive days (from 5 to 6 and 10 to 11 in April):

$$\Delta \langle \chi(\tilde{\varphi}, t) \rangle_i^{\tilde{a}} = \int_{t_{\text{obs}}} \frac{dt}{t_{\text{obs}}} (\langle \chi(\tilde{\varphi}, t) \rangle_i^{2\tilde{a}-1} - \langle \chi(\tilde{\varphi}, t) \rangle_i^{2\tilde{a}}), \quad (9)$$

where $\tilde{a} = 1, 2$ denotes the \tilde{a} -th pair of images and $t_{\text{obs}} = 6$ hours accounts for the EHT’s imaging time on each observation day (note that the de facto imaging time on each day differs slightly, and the uniform choice of t_{obs} in (9) is taken for convenience.). This design is intended to mitigate the impacts of temporal variation in the accretion disk over longer time scales. The posterior distribution of $\log_{10} \varepsilon$ for a given DP mass μ is then given by $P(\log_{10} \varepsilon | \{\Delta \langle \chi(\tilde{\varphi}, t) \rangle_i^{\tilde{a}}\}, \mu)$. In the analysis, the “ i ” is

restricted to the $\tilde{\varphi}$ bins that are approximately Gaussian, ensuring $\langle\chi\rangle$ to be well reconstructed [34].

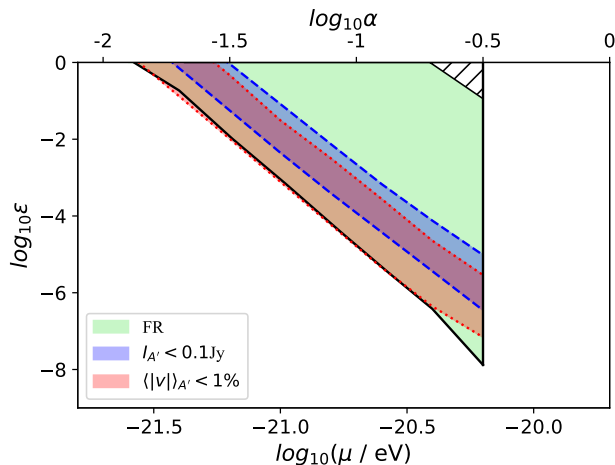


FIG. 1: 95% CL exclusion limits on the photon-DP kinetic mixing parameter ε , using the EHT polarimetric images of the M87*. The green shaded region has been excluded by the image FR observation. The blue and red shaded regions are excluded by the observations of image intensity and dichroism, assuming a precision of current EHT level. In the hatched region, the IPOLE calculation becomes not reliable, since the radiative transfer coefficients in Eq. (6) are computed in IPOLE by employing the public SYMPHONY code [48], where numeric fitting functions are used assuming $\nu \gg \nu_B$.

We demonstrate in Fig. 1 the 95% CL FR limits on the photon-DP kinetic mixing parameter ε , using the EHT polarimetric images of the M87*. Here we have assumed flat priors for $\log_{10} \varepsilon$ and the constant phase ϕ_0 and marginalised the latter away. The analysis is restricted to $\alpha < 0.3$ to meet the superradiance condition for the considered DP cloud mode of $(n, j, l, m) = (1, 1, 0, 1)$ [55]. These limits approximately scale with the DP mass as $\sim \mu^{11/2}$. For $\nu \gg \nu_B$, the DP-induced FR is $\sim \int dl n_e \mathcal{B}_{A'}$, with the integration performed along the light trajectory. Since the integrand is proportional to $\mathcal{B}_{A'} \propto B_{A'} \propto \varepsilon \alpha^{11/2}$, such scaling behavior is expected for a given precision of the FR measurement. Notably, as the cadence of $\Delta T = 1$ day for the analyzed image pairs represents a fraction of $\Delta T/T_{\text{osc}}$ of the full signal oscillation period, the signal magnitude will be reduced for $\mu \lesssim 10^{-20}$ eV where $\Delta T/T_{\text{osc}}$ becomes $\lesssim 1$. However, such a reduction can be compensated for by a factor of $1/\omega$ brought in from performing the integration of $\int dl$, which yields a signal magnitude $\sim \frac{1}{\omega} \times \frac{\Delta T}{T_{\text{osc}}} \propto \Delta T$. This implies that, if the four M87* images are paired with a longer cadence, or the M87* is imaged over a longer period later, the exclusion limits from the FR observation could be enhanced in the considered mass range.

Besides Q and U , the Stokes parameters I and V are also subject to influence by the DP-induced magnetic field and hence can be applied as a probe for the DP. As a demonstration, let us consider two EHT observables.

One is total compact flux density of the images F_{cpct} and has been measured with a precision of ~ 0.1 Jy at the EHT [56]. Another one is average fractional circular polarization $\langle|V|\rangle = \int d\sigma |V| / \int d\sigma |I|$, where $\int d\sigma$ denotes an integration over the M87* image. The EHT precision of measuring $\langle|V|\rangle$ is currently $\sim 10^{-2}$ [57]. To estimate the sensitivity potential of these two observables, we require the magnitude of the $\mathcal{B}_{A'}$ -induced oscillations in these two observables to be smaller than their measurement precisions. The excluded parameter regions are also displayed in Fig. 1, as blue and red shaded bands, respectively. Different from the FR analysis above, we have not considered temporal variation of the measured values over the observation period here. These results thus should be interpreted as “projected limits” based on the current EHT precision level.

These exclusion limits of ε demonstrate a feature of scaling with $\mu^{11/2}$, consistent with our expectation. However, the exclusion power of F_{cpct} and $\langle|V|\rangle$ become relatively weak for a strong $\vec{\mathcal{B}}_{A'}$ field, yielding an exclusion band in both cases. This outcome is caused by the variation of $|dI/d\mathcal{B}|$ and $|dV/d\mathcal{B}|$ as the $\mathcal{B}_{A'}$ or the \mathcal{B} increases. As a qualitative discussion, we can turn off the Faraday mixing coefficients and decouple the V parameter from the radiative transfer equation. Then for homogeneous and thermal plasma [58] we have $I = f_\nu [2 - \exp(-(\alpha_I + \alpha_Q)L) - \exp(-(\alpha_I - \alpha_Q)L)]$, where L is plasma thickness. Then we can find $|dI/d\mathcal{B}| \propto \mathcal{B}^{-4/3}$ for weak \mathcal{B} , and exponentially suppressed for $(\alpha_I \pm \alpha_Q)L \gtrsim 1$ where \mathcal{B} becomes relatively strong and I gets saturated. Similarly, the Faraday mixing parameter ρ_Q , which is key for rotating the U parameter to the V parameter, is proportional to \mathcal{B}^2 for small \mathcal{B} while becomes exponentially suppressed as \mathcal{B} becomes large. The exclusion band obtained from measuring $\langle|V|\rangle$ thus gets explained. In conclusion, all of these polarimetric observables have roughly comparable sensitivities at the EHT in probing for the photon-DP mixing parameter if this parameter is relatively small or the DP-induced $\vec{\mathcal{B}}_{A'}$ is relatively weak.

SUMMARY AND OUTLOOK

In this Letter, we have proposed and developed the DP polarimetry as a universal methodology to detect the DP. As a demonstration, we applied this methodology to search for the ultralight DP produced through the superradiance near supermassive BHs. Then using the polarimetric measurements of the radiation from the M87* at the EHT, we showed that all Stokes parameters can probe for and set novel limits on the photon-DP kinetic mixing parameter.

Besides improving the sensitivity analysis in this proof-of-concept study, several significant scientific tasks can be readily recognized for next-step explorations. For

example, we can extend this analysis to probe a high-mass region of the ultralight DP by incorporating additional data like the Sagittarius A* images [59]. Moreover, we can generalize the application of the DP polarimetry for the DP detection to the laboratory polarimetric experiments and other astronomical or cosmological polarimetric observations. Finally, an effective current can be induced also by the axion Chern-Simons coupling in the Maxwell's equations, enriching the axion polarimetry. Different from its DP counterpart, this current is proportional to the existing magnetic field strength. We leave these explorations to future work.

Note Added: When this Letter was in finalization, the paper [60] appeared on arXiv. Although this paper aims to address the detection of the ultralight DP also, it employs a completely different method based on the DP interactions with charged particles (inverse Compton scattering).

Acknowledgments

We would thank Yifan Chen, Shuo Xin and Yue Zhao for useful discussions, and the Center for High Throughput Computing at the University of Wisconsin-Madison for providing computing resources [61]. J.R. is supported in part by the National Natural Science Foundation of China under Grant No. 12275276. The HKUST team is supported by the Collaborative Research Fund under Grant No. C6017-20G which is issued by Research Grants Council of Hong Kong S.A.R.

* Electronic address: ftyleung@connect.ust.hk

† Electronic address: taoliu@ust.hk

‡ Electronic address: lusida1992@gmail.com

§ Electronic address: renjing@ihep.ac.cn

¶ Electronic address: ckkyue@connect.ust.hk

** Electronic address: kzhengae@connect.ust.hk

- [1] F. Zwicky, *Helv. Phys. Acta* **6**, 110 (1933).
- [2] N. Aghanim et al. (Planck), *Astron. Astrophys.* **641**, A6 (2020), [Erratum: *Astron. Astrophys.* 652, C4 (2021)], 1807.06209.
- [3] M. Markevitch, A. H. Gonzalez, D. Clowe, A. Vikhlinin, L. David, W. Forman, C. Jones, S. Murray, and W. Tucker, *Astrophys. J.* **606**, 819 (2004), [astro-ph/0309303](https://arxiv.org/abs/astro-ph/0309303).
- [4] E. Aprile et al. (XENON), *Phys. Rev. Lett.* **131**, 041003 (2023), 2303.14729.
- [5] Y. Meng et al. (PandaX-4T), *Phys. Rev. Lett.* **127**, 261802 (2021), 2107.13438.
- [6] J. Aalbers et al. (LZ), *Phys. Rev. Lett.* **131**, 041002 (2023), 2207.03764.
- [7] L. Hui, *Ann. Rev. Astron. Astrophys.* **59**, 247 (2021), 2101.11735.
- [8] J. Redondo and G. Raffelt, *JCAP* **08**, 034 (2013), 1305.2920.
- [9] N. Bar, K. Blum, J. Eby, and R. Sato, *Phys. Rev. D* **99**, 103020 (2019), 1903.03402.
- [10] H.-Y. Schive, T. Chiueh, and T. Broadhurst, *Nature Physics* **10**, 496–499 (2014), ISSN 1745-2481, URL <http://dx.doi.org/10.1038/nphys2996>.
- [11] W. Hu, R. Barkana, and A. Gruzinov, *Phys. Rev. Lett.* **85**, 1158 (2000), [astro-ph/0003365](https://arxiv.org/abs/astro-ph/0003365).
- [12] R. Hlozek, D. J. E. Marsh, and D. Grin, *Mon. Not. Roy. Astron. Soc.* **476**, 3063 (2018), 1708.05681.
- [13] M. Nori, R. Murgia, V. Iršič, M. Baldi, and M. Viel, *Mon. Not. Roy. Astron. Soc.* **482**, 3227 (2019), 1809.09619.
- [14] E. Braaten, A. Mohapatra, and H. Zhang, *Phys. Rev. Lett.* **117**, 121801 (2016), 1512.00108.
- [15] B. Holdom, *Phys. Lett. B* **166**, 196 (1986).
- [16] R. Bähre et al., *JINST* **8**, T09001 (2013), 1302.5647.
- [17] P. Agnes et al. (DarkSide), *Phys. Rev. Lett.* **130**, 101002 (2023), 2207.11968.
- [18] E. Aprile et al. (XENON), *Phys. Rev. D* **106**, 022001 (2022), [Erratum: *Phys. Rev. D* 110, 109903 (2024)], 2112.12116.
- [19] R. Cervantes et al., *Phys. Rev. D* **106**, 102002 (2022), 2204.09475.
- [20] H. An, S. Ge, W.-Q. Guo, X. Huang, J. Liu, and Z. Lu, *Phys. Rev. Lett.* **130**, 181001 (2023), 2207.05767.
- [21] A. Caputo, H. Liu, S. Mishra-Sharma, and J. T. Ruderman, *Phys. Rev. Lett.* **125**, 221303 (2020), 2002.05165.
- [22] D. Wadekar and G. R. Farrar, *Phys. Rev. D* **103**, 123028 (2021), 1903.12190.
- [23] S. Yan, L. Li, and J. Fan, *JHEP* **06**, 028 (2024), 2312.06746.
- [24] A. Caputo, A. J. Millar, C. A. J. O'Hare, and E. Vitagliano, *Phys. Rev. D* **104**, 095029 (2021), 2105.04565.
- [25] D. J. E. Marsh, *Phys. Rept.* **643**, 1 (2016), 1510.07633.
- [26] L. Hui, J. P. Ostriker, S. Tremaine, and E. Witten, *Physical Review D* **95**, 043541 (2017).
- [27] S. M. Carroll, G. B. Field, and R. Jackiw, *Phys. Rev. D* **41**, 1231 (1990).
- [28] S. M. Carroll and G. B. Field, *Phys. Rev. D* **43**, 3789 (1991).
- [29] A. Lue, L.-M. Wang, and M. Kamionkowski, *Phys. Rev. Lett.* **83**, 1506 (1999), [astro-ph/9812088](https://arxiv.org/abs/astro-ph/9812088).
- [30] B. Feng, M. Li, J.-Q. Xia, X. Chen, and X. Zhang, *Phys. Rev. Lett.* **96**, 221302 (2006), [astro-ph/0601095](https://arxiv.org/abs/astro-ph/0601095).
- [31] M. A. Fedderke, P. W. Graham, and S. Rajendran, *Phys. Rev. D* **100**, 015040 (2019), 1903.02666.
- [32] T. Liu, X. Lou, and J. Ren, *Phys. Rev. Lett.* **130**, 121401 (2023), 2111.10615.
- [33] X. Xue et al. (2024), 2412.02229.
- [34] Y. Chen, Y. Liu, R.-S. Lu, Y. Mizuno, J. Shu, X. Xue, Q. Yuan, and Y. Zhao, *Nature Astronomy* **6**, 592–598 (2022), ISSN 2397-3366, URL <http://dx.doi.org/10.1038/s41550-022-01620-3>.
- [35] G.-W. Yuan, Z.-Q. Xia, C. Tang, Y. Zhao, Y.-F. Cai, Y. Chen, J. Shu, and Q. Yuan, *Journal of Cosmology and Astroparticle Physics* **2021**, 018 (2021).
- [36] Y. Chen, C. Li, Y. Mizuno, J. Shu, X. Xue, Q. Yuan, Y. Zhao, and Z. Zhou, *Journal of Cosmology and Astroparticle Physics* **2022**, 073 (2022).
- [37] X. Gan, L.-T. Wang, and H. Xiao, *Phys. Rev. D* **110**, 063039 (2024), 2311.02149.
- [38] A. Castillo, J. Martin-Camalich, J. Terol-Calvo, D. Blas, A. Caputo, R. T. G. Santos, L. Sberna, M. Peel, and J. A. Rubiño Martín, *JCAP* **06**, 014 (2022), 2201.03422.

- [39] S. Adachi et al. (POLARBEAR) (2024), 2403.02096.
- [40] S. L. Detweiler, *Phys. Rev. D* **22**, 2323 (1980).
- [41] K. Akiyama et al. (Event Horizon Telescope), *Astrophys. J. Lett.* **875**, L1 (2019), 1906.11238.
- [42] M. Baryakhtar, R. Lasenby, and M. Teo, *Physical Review D* **96**, 035019 (2017).
- [43] N. Siemonsen, C. Mondino, D. Egana-Ugrinovic, J. Huang, M. Baryakhtar, and W. E. East, *Phys. Rev. D* **107**, 075025 (2023), 2212.09772.
- [44] S. A. Teukolsky, *Phys. Rev. Lett.* **29**, 1114 (1972).
- [45] S. Xin and E. R. Most (2024), 2406.02992.
- [46] P. K. Leung, C. F. Gammie, and S. C. Noble, *Astrophys. J.* **737**, 21 (2011).
- [47] A. Marszewski, B. S. Prather, A. V. Joshi, A. Pandya, and C. F. Gammie, *The Astrophysical Journal* **921**, 17 (2021).
- [48] J. Dexter, *Mon. Not. Roy. Astron. Soc.* **462**, 115 (2016), 1602.03184.
- [49] A. Pandya, Z. Zhang, M. Chandra, and C. F. Gammie, *Astrophys. J.* **822**, 34 (2016), 1602.08749.
- [50] M. Moscibrodzka and C. F. Gammie, *Mon. Not. Roy. Astron. Soc.* **475**, 43 (2018), 1712.03057.
- [51] S. C. Noble, P. K. Leung, C. F. Gammie, and L. G. Book, *Class. Quant. Grav.* **24**, S259 (2007), astro-ph/0701778.
- [52] <https://github.com/AFD-Illinois/ipole>.
- [53] H.-Y. Pu and A. E. Broderick, *The Astrophysical Journal* **863**, 148 (2018).
- [54] K. Akiyama et al. (Event Horizon Telescope), *Astrophys. J. Lett.* **910**, L12 (2021), 2105.01169.
- [55] S. R. Dolan, *Phys. Rev. D* **76**, 084001 (2007), 0705.2880.
- [56] K. Akiyama et al. (Event Horizon Telescope), *Astrophys. J. Lett.* **875**, L4 (2019), 1906.11241.
- [57] K. Akiyama, A. Alberdi, W. Alef, J. C. Algaba, R. Anantua, K. Asada, R. Azulay, U. Bach, A.-K. Baczko, D. Ball, et al., *The Astrophysical Journal Letters* **957**, L20 (2023).
- [58] D. B. Melrose and R. C. McPhedran, *Electromagnetic Processes in Dispersive Media* (1991).
- [59] K. Akiyama et al. (Event Horizon Telescope), *Astrophys. J. Lett.* **964**, L25 (2024).
- [60] J. F. Acevedo, A. Bhoonah, and K. Cheng (2025), 2501.01489.
- [61] Center for High Throughput Computing, *Center for high throughput computing* (2006), URL <https://chtc.cs.wisc.edu/>.